



# Photobiomodulation with 808-nm diode laser light promotes wound healing of human endothelial cells through increased reactive oxygen species production stimulating mitochondrial oxidative phosphorylation

Andrea Amaroli<sup>1</sup> · Silvia Ravera<sup>2</sup> · Francesca Baldini<sup>3</sup> · Stefano Benedicenti<sup>1</sup> · Isabella Panfoli<sup>2</sup> · Laura Vergani<sup>3</sup>

Received: 8 March 2018 / Accepted: 16 August 2018  
© Springer-Verlag London Ltd., part of Springer Nature 2018

## Abstract

Photobiomodulation of cells using near-infrared (NIR) monochromatic light can affect cell functions such as proliferation, viability, and metabolism in a range of cell types. Evidence for the effects of near-infrared light on endothelial cells has been reported, but the studies were mainly performed using VIS light emitted by low-energy lasers, because NIR wavelengths seemed negatively stimulate these cells. Cell viability, free radical-induced oxidative stress, NF- $\kappa$ B activation, nitric oxide release, mitochondrial respiration, and wound healing repair were assessed in human endothelial cells (HECV) irradiated with 808-nm diode laser light (laser setup = 1 W/cm<sup>2</sup>, 60 s, 60 J/cm<sup>2</sup>, CW vs measured energy parameter = 0.95 W/cm<sup>2</sup>, 60 s, 57 J/cm<sup>2</sup>, mode CW) emitted by an handpiece with flat-top profile. No difference in viability was detected between controls and HECV cells irradiated with 808-nm diode laser light for 60 s. Irradiated cells demonstrated higher proliferation rate and increased migration ability associated to moderate increase in ROS production without a significant increase in oxidative stress and oxidative stress-activated processes. Near-infrared light stimulated mitochondrial oxygen consumption and ATP synthesis in HECV cells. Short near-infrared irradiation did not affect viability of HECV cells, rather led to a stimulation of wound healing rate, likely sustained by ROS-mediated stimulation of mitochondrial activity. Our results demonstrating that near-infrared led to a shift from anaerobic to aerobic metabolism provide new insight into the possible molecular mechanisms by which photobiomodulation with 808-nm diode laser light protects against inflammation-induced endothelial dysfunction, seemingly promising to enhance their therapeutic properties.

**Keywords** Photobiomodulation (PBM) · NIR-diode laser · Human endothelial cells (HECV) · Mitochondrial respiration · Wound regeneration

## Introduction

In the USA alone, experts estimated that the number of chronic wounds exceeds two million and perhaps up to five million

annually. Wound healing is a complex process that involves a large number of cell types and requires a dynamic angiogenic response to create new capillary beds. In fact, impaired angiogenic response is associated with poorly healing outcomes.

✉ Andrea Amaroli  
andrea.amaroli.71@gmail.com

Silvia Ravera  
silvia.ravera@gmail.com

Francesca Baldini  
baldinifrancesca92@gmail.com

Stefano Benedicenti  
benedicenti@unige.it

Isabella Panfoli  
Isabella.Panfoli@unige.it

Laura Vergani  
Laura.Vergani@unige.it

<sup>1</sup> Department of Surgical Sciences and Integrated Diagnostic, University of Genoa, Largo R. Benzi 10, 16132 Genoa, Italy

<sup>2</sup> Department of Pharmacy, Biochemistry Laboratory, University of Genoa, Viale Cembrano 4, 16147 Genoa, Italy

<sup>3</sup> Department of Earth, Environmental and Life Sciences, University of Genoa, Corso Europa 26, 16132 Genoa, Italy

Endothelial cell dysfunction is a significant contributor to impaired wound healing which occurs in many diseases such as inflammation-related diseases, including atherosclerosis, vasculopathy, ischemia-reperfusion injury, hypertension, heart failure, and diabetes. The general therapies for wound ulcer involve the combination of debridement, topical western medications, and intravenous administration of drugs. Recently, the possible use of light irradiation for wound ulcer therapy has been proposed [1].

Low-level laser therapy (LLLT), also known as photobiomodulation (PBM), is an emerging therapeutic approach in which cells or tissues are exposed to low-power lasers or light-emitting diodes (LEDs) in the range of visible (VIS, 400–700 nm) and near-infrared (NIR, 700–1000 nm) wavelengths. These light sources are referred to as “low-level” in alternative to “high-power” lasers that are harmful for their important photothermal effects, whereas PBM acts rather through photochemical and photomechanical mechanisms [2].

Light is composed of photons whose energy depends on their wavelength; photons transfer their energy to specific organic molecules, called chromophores. The main cellular targets of PBM include cytochrome c oxidase (Cox) in mitochondria [3] and calcium ( $\text{Ca}^{2+}$ ) channels in plasma membranes, which seem to be affected by NIR laser light [4, 5]. For many years, action of PBM was essentially considered as depending on light-mitochondria interactions, likely through a stimulation of mitochondrial respiration and consequent production of reactive oxygen species (ROS) [3]. There is a tight relationship between ROS release, mainly by mitochondria, and  $\text{Ca}^{2+}$  signaling, with ROS regulating  $\text{Ca}^{2+}$  signaling and  $\text{Ca}^{2+}$  signaling affecting mitochondrial activities and ROS production [6]. Moreover, PBM was shown to stimulate collagen production [7], promote DNA [8] and protein [9] synthesis, increase ATP content [10], modulate cell migration and proliferation [9], accelerate tissue repair [11] and induce stem cell differentiation [12].

Most in vitro studies on PBM employed VIS light (600–700 nm) to stimulate keratinocytes and fibroblasts [13], and only few studies used endothelial cells [1, 14]. Moreover, endothelial cells were usually stimulated by VIS light emitted by low-energy lasers because, unlike keratinocytes and fibroblasts, they seemed to be not responsive to NIR wavelength [15]. The World Association of Laser Therapy (WALT, [www.walt.nu](http://www.walt.nu)) suggests to use fluences lower than  $10 \text{ J/cm}^2$ , by  $< 100 \text{ mW}$ , because higher fluences may damage DNA and other biopolymers [16]. However, both light absorption and scattering are elevated for VIS radiation, with consequent reduction of penetration, whereas the penetration depth increases for NIR, being maximal at about 810 nm [9]. Only limited evidences suggest that VIS light can be applied on deep tissues with the same efficiency from in vitro cells to in vivo organisms [9].

Recently, in order to improve light penetration, irradiation homogeneity, and procedure simplicity, handpiece with flat-top beam profile (flat-top handpiece) has been developed. This device has been tested on *Paramecium primaurelia* in previous studies from our group, which demonstrated that 808-nm diode laser light ( $1 \text{ W}$ ,  $1 \text{ W/cm}^2$ ,  $60 \text{ J}$ ,  $60 \text{ s}$ ,  $60 \text{ J/cm}^2$ , continuous-wave mode CW) increased mitochondrial activity and ATP production [17],  $\text{O}_2$  consumption [18], modulated  $\text{Ca}^{2+}$  fluxes [4], and cell fission rates [19]. Studies have also reported the effects of PBM on wound repair [1, 13, 14], but the molecular mechanisms underlying action of PBM are still unclear.

The aim of the present study was to elucidate the protective and stimulating effects of PBM using NIR light on in vitro cultured endothelial cells and to better understand the molecular mechanisms sustaining these effects. The 808-nm diode laser light at higher-fluence and –power energy (laser setup =  $1 \text{ W}$ ,  $1 \text{ W/cm}^2$ ,  $60 \text{ J}$ ,  $60 \text{ s}$ ,  $60 \text{ J/cm}^2$ , CW vs measured energy parameter =  $0.95 \text{ W}$ ,  $0.95 \text{ W/cm}^2$ ,  $57 \text{ J}$ ,  $60 \text{ s}$ ,  $57 \text{ J/cm}^2$ , mode CW) with flat-top handpiece was employed to treat human vascular endothelial cells (HECV) and to evaluate the effects at the molecular and cellular level. Overall, results indicate that PBM with NIR light stimulates wound healing in cultured endothelial cells via the shift from anaerobic to aerobic metabolism and the increase in  $\text{O}_2$  consumption and the ATP synthesis.

## Material and methods

### Chemicals

All chemicals, unless otherwise indicated, were of analytical grade and were supplied by Sigma-Aldrich Corp. (Milan, Italy).

### Cell cultures

The human endothelial cell line (HECV) isolated from umbilical vein was supplied by Cell Bank and Culture (GMP-IST—Genoa, Italy). Cells were grown in a humidified atmosphere with 5%  $\text{CO}_2$  at  $37 \text{ }^\circ\text{C}$  in Dulbecco’s modified Eagle’s medium high glucose (D-MEM) supplemented with L-glutamine and 10% FCS [20]. For treatments, cells were grown until 80% confluence, then incubated overnight (O/N) in starvation medium (serum-free medium with 0.25% bovine serum albumin—BSA).

### Irradiation experiments

For NIR irradiation, the 808-nm diode laser with the AB2799 handpiece (Doctor Smile—LAMBDA Spa—Vicenza, Italy) was utilized. According to the technical data ([http://www.doctor-smile.com/assests/prodotti/accessori/pdf/ST\\_](http://www.doctor-smile.com/assests/prodotti/accessori/pdf/ST_)

FLATTOP\_EN.pdf), the AB2799 handpiece with a flat-top profile allows a more homogenous irradiation over  $1 \text{ cm}^2$  surface area. This device is able to guarantee the same irradiation spot area ( $\sim 1 \text{ cm}^2$ ) and the same energy density from the contact point to 105 cm of distance from the target, different from the Gaussian profile irradiation of a standard handpiece where distribution of energy is inversely proportional to the tip-to-tissue distance [17]. As shown in Table 1, the laser energy was experimentally measured by using a power meter (ThorLabs, Dachau, Germany) and by keeping the AB2799 handpiece fixed in contact mode (Table 1A), at 3 mm (Table 1B), or at 50 cm (Table 1C) of distance from the power meter. The measurements were also performed in the presence of a plastic Petri dishes containing or not the cell culture medium (about 3 mm of depth) with the handpiece at 3 mm and 50 cm of distance from the power meter.

For irradiation experiments, HECV cells were cultured in 5-cm plastic Petri dishes. To maximize the effectiveness of laser treatment and avoid energy dispersion during irradiation, the cells were cultured in the center of the dishes (area =  $\sim 1 \text{ cm}^2$ ) and the dishes were wrapped in an aluminum foil with a central hole of a  $1 \text{ cm}^2$  of area (about the same size of the laser spot area), to avoid energy dispersion [12] (Table 1D). Then, the laser device was kept vertically in contact with the aluminum foil, in correspondence of the hole, at about 1-cm distance from the cell monolayer (Table 1B). In most experiments, HECV cells were irradiated with the 808-nm diode laser light (Wiser; Doctor Smile—Vicenza, Italy) emitted by the flat-top handpiece using 1 W of power energy,  $1 \text{ W/cm}^2$  of power density, single dose of 60 J, irradiation of 60 s, fluence of  $60 \text{ J/cm}^2$ , mode CW (corresponding to the measured laser therapy of 0.95 W,  $0.95 \text{ W/cm}^2$ , 57 J, 60 s,  $57 \text{ J/cm}^2$ , mode

**Table 1** Design of the laser irradiation for the experimental setup with HECV cell cultures

<b>TAB. 1. Design of the laser irradiation for the experimental setup with HECV cell cultures</b>						
<b>A</b> 	<b>B</b> 	<b>C</b> 	<b>D</b> 			
<b>Measured energy</b> 1.010±0.006 W	<b>Measured energy</b> 1.013±0.007 W	<b>Measured energy</b> 1.012±0.004 W				
<b>The table below shows the laser energy setup and the measured effective energy arriving to the HECV cells</b>						
	<b>Power energy</b>	<b>Power density</b>	<b>Time</b>	<b>Fluence</b>	<b>Dose</b>	<b>Mode</b>
<b>808nm setup Laser Therapy</b>	1 W	$1 \text{ W/cm}^2$	60 s	$60 \text{ J/cm}^2$	60 J	Continuous wave
<b>808nm measured Laser Therapy</b>	0.95 W	$0.95 \text{ W/cm}^2$	60 s	$57 \text{ J/cm}^2$	67 J	Continuous wave

CW (Table 1). In order to assess the effect of 808-nm laser light irradiation on cell viability, also longer irradiations were performed (100 s and 150 s) corresponding to a final fluences of 100 J/cm<sup>2</sup> and 150 J/cm<sup>2</sup>, respectively. Depending on the investigation performed the irradiated cells and the relative controls were analyzed immediately after the irradiation or at increasing periods up to 72 h.

### Evaluation of cell viability

Viability of HECV cells at 24 h, 48 h, and 72 h after irradiation compared to control was assessed by using the MTT (3-(4,5-dimethylthiazol-2-yl)-2,5-diphenyltetrazolium bromide) assay [21]. The assay was performed in six replicates using 96-well flat-bottomed culture plates (Sarstedt, Nümbrecht, Germany) as previously described [22]. Briefly, 2000 cells/well were seeded. After 24 h the cells were irradiated as above described. At the end of treatments, 0.02 ml/well of MTT solution (5 mg/mL in phosphate buffered saline-PBS) was added to the medium and incubated at 37 °C for 3 h. After removing the MTT solution, 0.2 ml/well of acidified isopropanol was added, and after agitation for 10 min at room temperature, absorbance at 570 nm was recorded in a microplate reader using a Varian Cary 50 Bio spectrophotometer (Agilent, Milan, Italy). Data are means ± S.D. of at least three independent experiments.

### Protein quantification

The protein content was determined by the bicinchoninic acid (BCA) method using BSA as the standard [23]. The BCA assay led to the formation of a complex with absorbance maximum at 562 nm that was quantified by using a Varian Cary 50 spectrophotometer (Agilent, Milan, Italy).

### Determination of lipid peroxidation

In control and irradiated HECV cells, lipid peroxidation was assessed 30 min and 1 h after irradiation by using the thiobarbituric acid reactive substances (TBARS) assay as previously described [24]. This spectrophotometric assay is based on the reaction of malondialdehyde (MDA; 1,1,3,3-tetramethoxypropane) with thiobarbituric acid (TBA) [25]. Briefly, 1 vol. of cell suspension was incubated for 45 min at 95 °C with 2 vol of TBA solution (0.375% TBA, 15% trichloroacetic acid, 0.25 N HCl). Then, 1 vol. of N-butanol was added and the absorbance of organic phase was read at 532 nm in a Varian Cary 50 spectrophotometer at 25 °C using Peltier-thermostated cuvette holder. MDA levels were expressed as pmol MDA/ml/mg protein. Protein content in the samples was determined by the BCA method. Data are means ± S.D. of at least three independent experiments.

### Determination of nitrite/nitrate (NOx) levels

In lysates of both control and irradiated HECV cells NO production was assessed at 1 h and 24 h after irradiation by spectrophotometric measurement of the end products, nitrites and nitrates, using the Griess reaction [26]. NO was detected by formation of a red pink color upon treatment of a NO<sub>2</sub><sup>-</sup>-containing sample with the Griess reagent. Nitrite accumulation (μmol NaNO<sub>2</sub>/mg sample protein) was calculated against a standard curve of sodium nitrite (NaNO<sub>2</sub>). All spectrophotometric analyses were carried out at 25 °C recording absorbance at 540 nm with spectrophotometer. Protein content in the samples was determined by the BCA method. Data are means ± S.D. of at least four independent experiments.

### In vitro scratch-wound healing assay

Migration of irradiated HECV cells compared to control cells was assessed by using the wound healing assay [27]. HECV cells were incubated until confluence was reached, then starved for 24 h. The cell monolayer was scraped with a p100 pipet tip making two crossing straight lines to create a “scratch” and some sample cells were irradiated as previously described [20]. Two views on the cross were photographed on each well (irradiated and control) attached to the microscope at × 4 magnification. Set of images were acquired at 6 h and 24 h and 30 h. To determine the migration of HECV, images were analyzed using ImageJ free software (<http://imagej.nih.gov/ij/>). The percentage of the closed area was measured and compared with the value obtained before treatment. An increase of the percentage of closed area indicated the migration of cells. Data are means ± S.D. of at least three independent experiments.

### Western blotting

Cells were irradiated by two different exposure protocols: 60 or 150 s, then scraped 1 h after irradiation beginning. Protein level of NF-κB p65 was assessed by Western blot analysis in control and irradiated HECV cells following a protocol previously described [24]. Briefly, the cellular pellet was suspended in 400 μL ice-cold Buffer A (20 mM Tris-HCl pH 7.8, 50 mM KCl, 10 μg/mL leupeptin, 0.1 mM dithiothreitol—DTT, 1 mM phenylmethanesulfonyl fluoride—PMSF); then 400 μL buffer B (buffer A plus 1.2% Nonidet P40) was added. The suspension was vortex-mixed for 10 s; after centrifugation (14,000×g for 30 s, 4 °C) the supernatant was discarded and the nuclear pellet was washed with 400 μL buffer A and centrifuged. The nuclear pellet was suspended in 100 μL buffer B, mixed thoroughly on ice for 15 min and finally centrifuged (14,000×g for 20 min, 4 °C). The supernatant containing the nuclear extracts was collected and the protein content in the samples was determined by the BCA

method. About 40- $\mu$ g proteins were electrophoresed on 12% sodium dodecyl sulfate polyacrylamide gel electrophoresis (SDS-PAGE) [28]. Membranes were blocked for 1 h in 5% fat-free milk/PBS (pH 7.4) and probed using rabbit anti-human NF- $\kappa$ B p65 (SC-109) antibody supplied by Santa Cruz Biotechnology (DBA, Milan, Italy). Membranes were incubated overnight at 4 °C with primary antibody in PBST buffer (PBS with 0.1% Tween 20) [29] washed and incubated with horseradish peroxidase (HRP)-conjugated rabbit anti-mouse IgG (Sigma-Aldrich) in PBST for 1 h at room temperature. Immune complexes were visualized using an enhanced chemiluminescence Western blotting analysis system (Bio-Rad ChemiDoc XRS System). Films were digitized and band optical densities were quantified against the actin band using a computerized imaging system and expressed as relative optical density (ROD, arbitrary units). ROD of each band was expressed as percentage respect to control.

### Oxygen consumption measurements

Oxygen consumption of control and irradiated HECV cells was measured at 37 °C in a closed chamber, immediately after irradiation and 30 min, 1 h, 2 h, 4 h, 6 h, and 24 h after irradiation, using an amperometric electrode (Unisense Microrespiration, Unisense A/S, Denmark). Briefly, 200,000 cells were permeabilized with 0.03 mg/ml digitonin for 1 min, centrifuged for 9 min at 1000 rpm, and resuspended in a buffer containing 137 mM NaCl, 5 mM KCl, 0.7 mM  $\text{KH}_2\text{PO}_4$ , 25 mM Tris-HCl, pH 7.4, and 25 mg/ml ampicillin. The same solution was used in the oxymetric measurements. Ten millimolars pyruvate plus 5 mM malate were added to stimulate the pathway composed by complex I, III, and IV. Twenty millimolars succinate was added to stimulate the pathway formed by complex II, III, and IV. To observe the ADP-stimulated respiration rates, 0.1 mM ADP was added after pyruvate and malate or succinate addition. To verify whether oxygen consumption was really due to the electron transport chain 0.1 mM rotenone or 50  $\mu$ M antimycin A, specific inhibitors of complex I or complex III, respectively, were used (data not shown). The respiratory rates were expressed as nmol O/min/ $10^6$  cells [30].

### ATP synthase activity assay

ATP production was measured at 37 °C in both control and irradiated cells, immediately after irradiation and 30 min, 1 h, 2 h, 4 h, 6 h, and 24 h after irradiation. To evaluate the ATP synthase activity, 100,000 cells were incubated for 10 min at 37 °C in a medium containing: 10 mM Tris-HCl, pH 7.4, 100 mM KCl, 5 mM  $\text{KH}_2\text{PO}_4$ , 1 mM EGTA, 2.5 mM EDTA, and 5 mM  $\text{MgCl}_2$ , 0.6 mM ouabain and 25 mg/ml ampicillin. Afterwards, ATP synthesis was induced by the addition of 10 mM pyruvate plus 5 mM malate or 20 mM

succinate, to stimulate the pathways composed by complexes I, III, and IV pathway or complexes II, III, and IV, respectively. The reaction was monitored for 2 min, every 30 s, in a luminometer (GloMax® 20/20n Luminometer, Promega Italia, Milano, Italy), by the luciferin/luciferase chemiluminescent method, with ATP standard solutions between  $10^{-8}$  and  $10^{-5}$  M (luciferin/luciferase ATP bioluminescence assay kit CLSII, Roche, Basel, Switzerland). Data were expressed as nmol ATP produced/min/ $10^6$  cells.

The oxidative phosphorylation efficiency (P/O ratio) was calculated as the ratio between the concentration of the produced ATP and the amount of consumed oxygen in the presence of respiring substrates and ADP. When the oxygen consumption is completed devoted to the energy production, the P/O ratio should be around 2.5 and 1.5 after pyruvate + malate or succinate addition, respectively [31].

### Statistical analysis

RNA and protein data are expressed as means  $\pm$  S.D. of at least four independent experiments in triplicate. Statistical analysis was performed using ANOVA with Tukey's post-test (GraphPad Software, Inc., San Diego, CA, USA).

## Results

The energy delivered by the 808-nm laser device was experimentally assessed and did not show significant differences using different setup ( $1.010 \pm 0.006$  W in contact mode,  $1.013 \pm 0.007$  W at 3 mm and  $1.012 \pm 0.004$  W at 50 cm of distance from the power meter). In the presence of the empty Petri dish, laser energy showed a significant ( $p < 0.05$ ) decrease of about -5% for all handpiece-power meter distances (contact =  $0.964 \pm 0.005$  W; 3 mm =  $0.949 \pm 0.006$  W; 50 cm =  $0.961 \pm 0.004$  W). The decrease was even higher ( $p < 0.05$ ) when the Petri dish contained a 3-mm layer of culture medium (the energy decreased up to  $0.878 \pm 0.004$  W and  $0.890 \pm 0.005$  W at 3 mm and 50 cm from the Petri dish, respectively) (data not shown). Therefore, the effective energy arriving to the cell monolayer was approximately  $0.950 \pm 0.005$  W (Table 1).

### Effects of the 808-nm diode laser light on endothelial cell viability and proliferation

Exposure of HECV cells to 808-nm laser light for increasing times (60 s, 100 s, and 150 s) affected cell viability (Fig. 1a). Reduction in cell viability was time-dependent and reached its maximum (-39% with respect to control;  $p \leq 0.001$ ) in cells grown for 72 h after 150 s of irradiation (L150). On the other hand, while a slight damaging effect (-25% with respect to control;  $p \leq 0.001$ ) was observed in cells irradiated for 100 s (L100), and no significant reduction in cell viability was

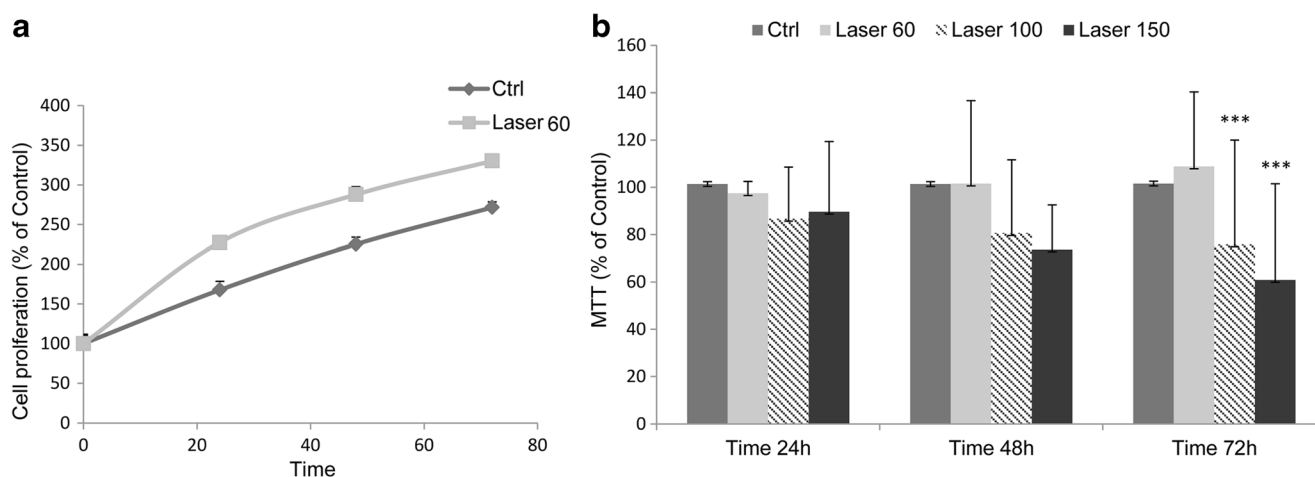


**Fig. 1** Effect of 808-nm diode laser light on viability and proliferation of endothelial cells. Effects of 808-nm diode laser light on HECV viability (a) and proliferation (b) were evaluated by the MTT assay. HECV cells were not irradiated (Ctrl) or irradiated with the 808-nm diode laser light for 60 (laser 60), 100 (laser 100), or 150 (laser 150) seconds. Data are

expressed as percent values with respect to controls. All values are mean  $\pm$  S.D. from at least three independent experiments. ANOVA followed by Tukey's test was used to assess the statistical significance between groups. Significant differences vs control (Ctrl) are denoted by symbol \*\*\* $p \leq 0.001$

measured for the shortest irradiation (60 s; L60) at all time points. Based on these results, for the subsequent experiments, we selected the irradiation time that does not affect cell viability. The shortest irradiation (60 s) not only did not reduce viability of HECV cells but stimulated their proliferation at all times analyzed (+36% at 24 h, +28% at 48 h; +22% at 72 h;  $p \leq 0.001$ ) (Fig. 1b).

### Effect of the 808-nm diode laser light on ROS and NO production in endothelial cells

Lipid peroxidation, one of the most common indicators of ROS-induced oxidative stress, was quantified in control (C) and HECV cells irradiated for 60 s (L60). The production of MDA was measured at different times after irradiation. We found that it markedly increased shortly after irradiation (30 min), slightly decreasing at 1 h after irradiation (+79% and +45% with respect to controls, respectively;  $p \leq 0.01$ ) (Fig. 2a).

Release of nitric oxide (NO), a major modulator of endothelial function, was quantified in control (C) and HECV cells irradiated for 60 s. Irradiated HECV cells showed a slight but not significant increase in NO release at both 30 min (data not shown), 1-h and 24-h time points after irradiation. Although slight, the extent of NO release was similar to that measured in HECV cells exposed for 24 h to a classical stimulator such as 2  $\mu\text{g/ml}$  of bacterial lipopolysaccharide (LPS) (Fig. 2b).

The activation of the transcription factor NF- $\kappa$ B, known to mediate the inflammatory responses to oxidative stress was also assessed. HECV cells irradiated with NIR light for both 60 s and 150 s showed a slight increase in the NF- $\kappa$ B p65 level which was not significant both 1 h and 24 h after irradiation with respect to control (Fig. 2c).

### Effect of the 808-nm diode laser light on aerobic metabolism of endothelial cells

The effect of 808-nm diode laser light on aerobic metabolism was assessed in control and irradiated HECV cells immediately after irradiation and 30 min, 1 h, 2 h, 4 h, 6 h, and 24 h after irradiation. The oxygen consumption and the ATP synthesis were evaluated as markers of mitochondrial oxidative phosphorylation (OXPHOS). As reported in Fig. 3, the oxygen consumption in untreated HECV was around  $13.9 \pm 1.2$  nmol O/min/ $10^6$  cell, a value that remained constant over the time (Fig. 3a). In irradiated HECV cells, the oxygen consumption was stimulated with respect to the control; it started to increase at 1 h after irradiation and reached the maximum at 4 h after irradiation. Then the oxygen consumption remained rather constant up to 24 h after irradiation (Fig. 3a). The same trend was observed analyzing the ATP synthesis, which started to increase at 1 h after irradiation reaching the maximum at 4 h (Fig. 3b).

Moreover, the P/O value, an index of OXPHOS efficiency, was around 2.5 for all the samples, indicating that the ATP synthesis and the oxygen consumption remained coupled [29] also after the laser treatment.

### Effects of the 808-nm diode laser on endothelial function

The effects of 808-nm laser light on migrating ability of HECV cells were evaluated using the wound healing assay (Fig. 4a, b). The microscopy images show that scratch closure occurred at a faster rate when HECV cells were irradiated for 60 s (L60) with 808-nm diode laser light, compared to controls (C). In detail, no significant differences in cell migration

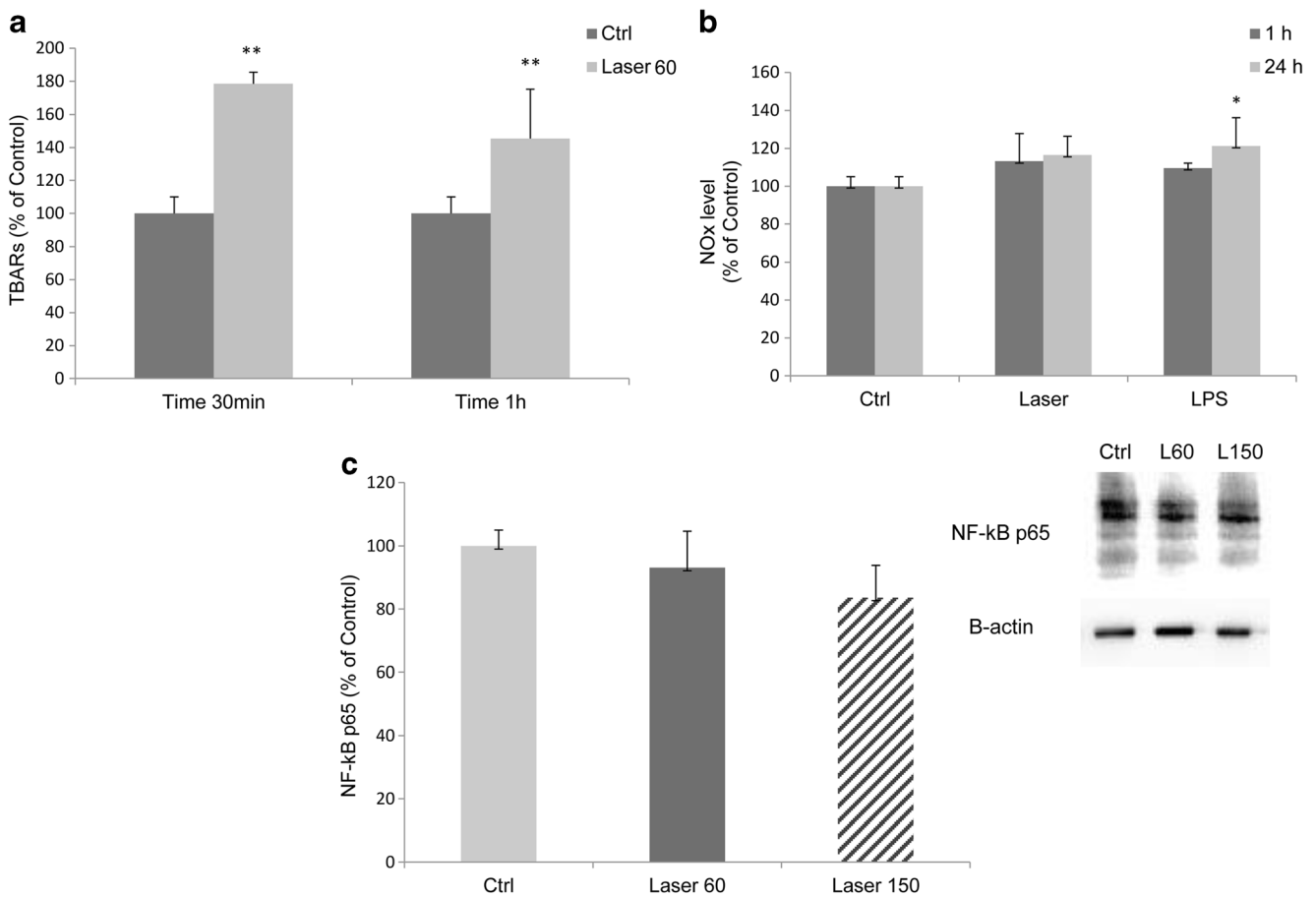


**Fig. 2** Effect of 808-nm diode laser light on ROS and NO production in endothelial cells. In HECV cells not irradiated (Ctrl) or irradiated for 60 s (laser 60) we quantified **a** the intracellular level of MDA (pmol MDA/ml  $\times$  mg of sample protein) at different times after irradiation (30 min, 1 h) using the TBARS assay. Data are expressed as percentage values with respect to controls and normalized for total protein. **b** The release of NO at different times after irradiation (1 h, 24 h). As comparison HECV cells were also stimulated for 24 h with 2  $\mu$ g/ml of LPS. Data are expressed as percentage values with respect to controls and normalized for total protein. **c** In HECV cells not irradiated or irradiated for both 60 s (laser

60) and 150 s (laser 150), the activation of the transcription factor NF- $\kappa$ B was assayed at 1 h and 24 h after irradiation. Densitometric analysis of nuclear NF- $\kappa$ B/p65 was evaluated by Western blotting;  $\beta$ -actin was the protein loading control used as housekeeping gene for normalization and data are expressed as percentage values with respect to controls. All values are mean  $\pm$  S. D. from at least three independent experiments. ANOVA followed by Tukey's test was used to assess the statistical significance between groups. Significant differences vs control (Ctrl) are denoted by symbols \*\*\* $p \leq 0.001$ , \*\* $p \leq 0.01$ , \* $p \leq 0.05$

rates were observed shortly after the scratch (6 h), whereas at longer times (24 and 30 h) the irradiated cells showed a more marked wound repair ability than control cells. At both 24 and 30 h after irradiation, the wound size was significantly reduced with respect to controls with an improvement in wound repair with respect to controls (+ 19% and + 10%, respectively;  $p < 0.001$ ).

## Discussion

The present report demonstrated that short irradiation of 60 s, by the laser setup of 1 W, 1 W/cm<sup>2</sup>, 60 J, 60 J/cm<sup>2</sup>, CW (real measured energy = 0.95 W, 0.95 W/cm<sup>2</sup>, 57 J, 57 J/cm<sup>2</sup>, CW), of human vascular endothelial cells in vitro with 808-nm diode laser light was able to stimulate endothelial cell

proliferation and oxidative metabolism, which resulted in a more efficient wound repair ability. These effects occurred without a marked stimulation of NO production, a modulator of endothelial function. In fact, it was observed that NIR irradiation only elicited a slight increase in NO release, namely of similar extent to that induced by exposure of HECV cells to LPS for 24 h. The proliferative and metabolic effects of NIR on endothelial cells were rather associated to moderate increase in ROS production, according to previous reports indicating that NIR light stimulates intracellular ROS release [32]. In detail, following short exposure to NIR, we observed a transient increase in lipid peroxidation, taken as a common indicator of ROS-induced oxidative stress. ROS production was maximal immediately after irradiation (30 min) and decreased thereafter. Interestingly, such a rapid and transient increase in ROS production was not able to activate NF- $\kappa$ B,

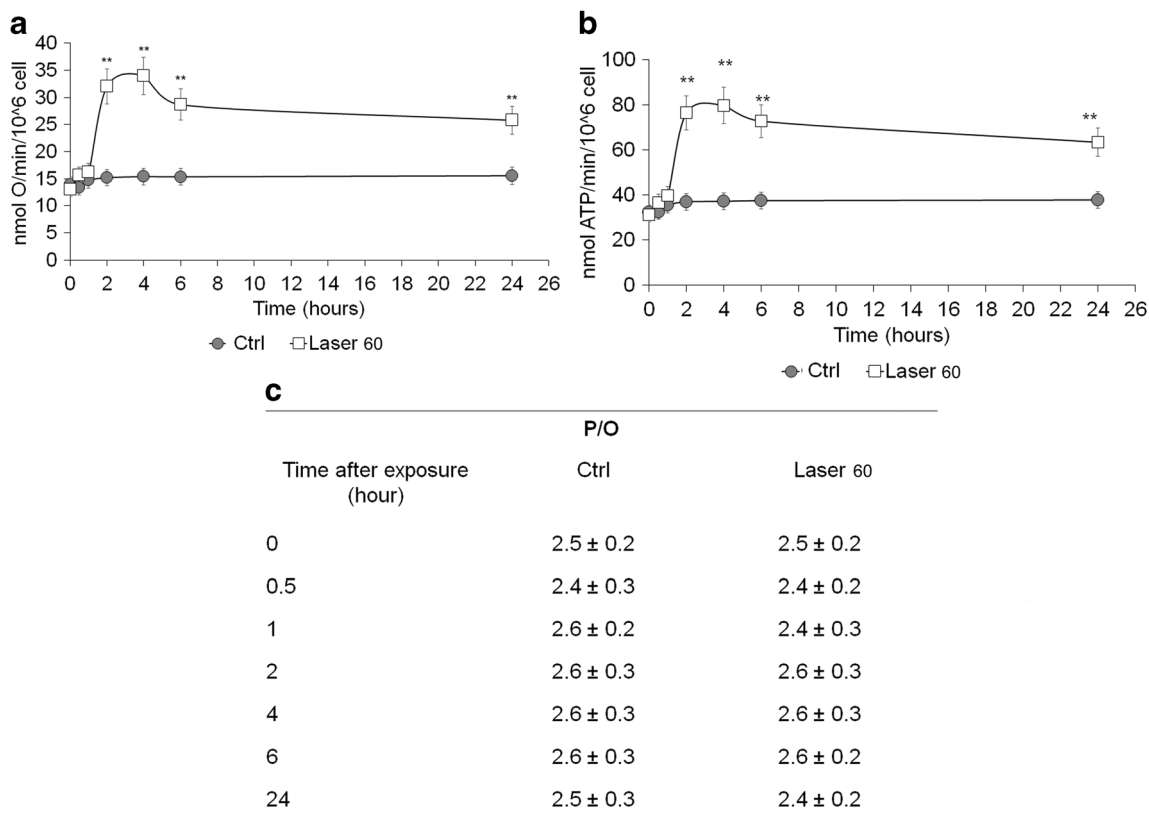


**Fig. 3** Effect of 808-nm diode laser light on aerobic metabolism of endothelial cells. Panels A and B compare the oxygen consumption and ATP synthesis, respectively, in HECV cells treated with laser (white square) or untreated (gray circle). The ability to consume oxygen and synthesize ATP was evaluated for several times after laser treatment (0, 0.5, 1, 2, 4, 6, and 24 h). Panel C reports the effectiveness of

mitochondrial respiration as the ratio between the ATP produced and the oxygen consumed (P/O ratio). Each panel is representative of three independent experiments and the data are expressed as mean ± S.D. \*\* indicates a significant difference for  $p < 0.01$  between the treated and untreated samples

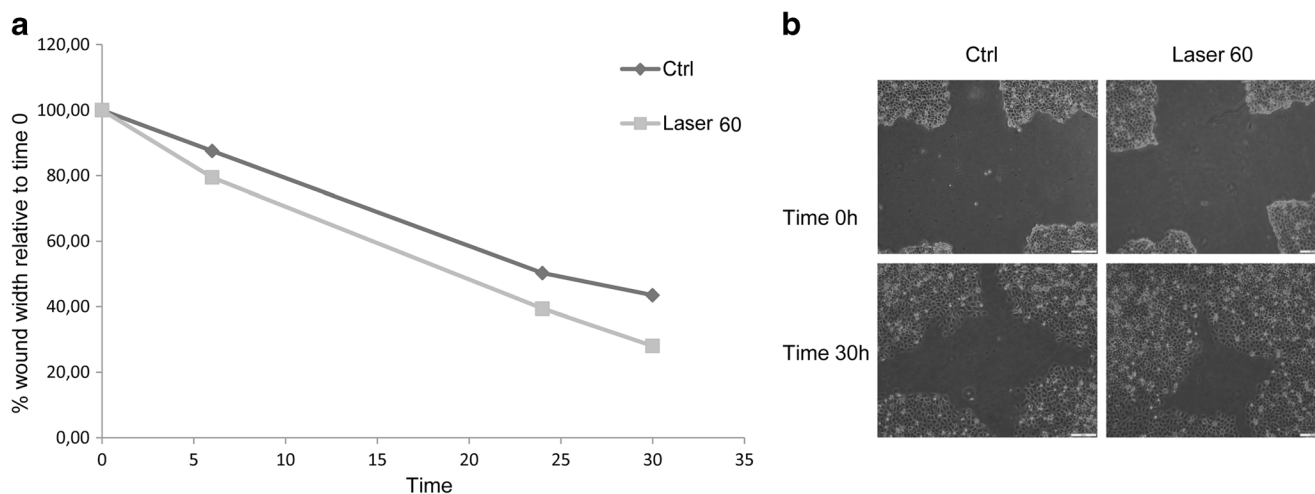


**Fig. 4** Effect of 808-nm diode laser light on migrating ability of endothelial cells. **a** In HECV cells, the cell migration was measured by the T scratch assay in control (Ctrl) and in cells irradiated for 60 s (laser 60). Slides were photographed at 6 h, 24 h, and 30 h after the scratch. T scratch assay representative images were shown (**b**). Graphs representing

the percentage of the closed area as compared to time = 0. Values are mean ± S. D. from at least three independent experiments. ANOVA followed by Tukey's test was used to assess the statistical significance between groups. Significant differences vs control (Ctrl) are denoted by symbols \*\*\* $p \leq 0.001$ , \*\* $p \leq 0.01$ , \* $p \leq 0.05$

one of the main target of ROS, which typically mediates the inflammatory response to oxidative stress by controlling cytokine production and intracellular signaling. Although previous studies reported a marked effect of NIR on ROS-induced activation of NF- $\kappa$ B [33], the discrepancy with our results can be due to different cellular types, irradiation fluences and procedures. In accordance with its bland induction of oxidative stress, short NIR irradiation did not alter significantly the endothelial cell viability; only longer (> 100 s) irradiation of HECV cells with NIR did affect cell viability to a certain extent. It is known that while prolonged exposure to high ROS concentrations may lead to various disorders, low ROS concentrations may exert beneficial effects regulating cell signaling cascades [34].

The present results indicate that the NIR treatment is able to augment aerobic metabolism, enhancing the O<sub>2</sub> consumption and the aerobic ATP synthesis. Notably, in basal conditions, endothelial cells are characterized by a high glycolytic rate and a rather low oxidative phosphorylation [35]. Such a metabolic choice apparently grants low basal ROS production, maintenance of a hypoxic environment, and elevated production of lactate which is a known pro-angiogenic factor [35]. The observed increase in ROS production after NIR irradiation may sustain the shift from anaerobic to aerobic metabolism, as demonstrated by the increased ATP synthesis, which is necessary for stimulation of cell proliferation. In accordance with our findings, previous reports showed that ATP can exert a selective mitogenic effect on different cell populations [36]. The stimulation of both O<sub>2</sub> consumption and aerobic ATP synthesis after 808-nm diode laser light irradiation suggests that NIR may act on HECV cells by improving electron transport efficiency. All these results are in accordance with the hypothesis that Cox in mitochondria may be one of the main targets of PBM. In fact, in isolated mitochondria, He-Ne laser irradiation has been shown to promote O<sub>2</sub> consumption and enhance electron transport to increase mitochondrial inner membrane potential and ATP synthesis by enhancing activity of Cox, the Complex IV of the respiratory chain [37]. We wish to emphasize that NIR irradiation did not play any uncoupling effect on mitochondria, as it did not alter the ratio between the ATP produced and the O<sub>2</sub> consumed (P/O ratio), this indicating that the treatment did not damage mitochondria.

Another possibility is that NIR light at power and energy inducing PBM might act indirectly on mitochondria by affecting Ca<sup>2+</sup> flows through plasma membrane and/or alter intracellular Ca<sup>2+</sup> concentration. In fact, as described by Brookes et al. [38], calcium may promote ATP synthesis by stimulating enzymes of the Krebs cycle and oxidative phosphorylation.

In conclusion, here, we demonstrate new insights on the molecular mechanisms sustaining the stimulation by NIR higher-fluence and -power energy on tissue repair. Since the wavelength of 808 nm has a high-deeper penetration, our PBM parameter stands as effective therapy for future in vivo

investigations and may contribute in many biomedical approaches to augment the success of regenerative medicine.

**Acknowledgments** We thank Dr. Milena Regazzoni for her support in the experimental activity. A special thanks to Prof. Adriana Voci for the constant support and encouragement.

**Funding information** This research was supported by grants from University of Genova (Vergani FRA nos. 2015 and 2016).

## Compliance with ethical standards

**Conflict of interest** All authors declare that they have no conflict of interest.

## References

- Góralczyk K, Szymańska J, Lukowicz M, Drela E, Kotzbach R, Dubiel M, Michalska M et al (2015) Effect of LLLT on endothelial cells culture. *Lasers Med Sci* 30(1):273–278
- Khan I, Arany P (2015) Biophysical approaches for oral wound healing: emphasis on photobiomodulation. *Adv Wound Care (New Rochelle)* 4(12):724–737
- Karu T (2010) Mitochondrial mechanisms of photobiomodulation in context of new data about multiple roles of ATP. *Photomed Laser Surg* 28(2):159–160
- Amaroli A, Benedicenti A, Ferrando S, Parker S, Selting W, Gallus L, Benedicenti S (2016) Photobiomodulation by infrared diode laser: effects on intracellular calcium concentration and nitric oxide production of *Paramecium*. *Photochem Photobiol* 92(6):854–862
- Wang Y, Huang YY, Wang Y, Lyu P, Hamblin MR (2016) Photobiomodulation (blue and green light) encourages osteoblastic-differentiation of human adipose-derived stem cells: role of intracellular calcium and light-gated ion channels. *Sci Rep* 6:33719
- Görlach A, Bertram K, Hudecova S, Krizanova O (2015) Calcium and ROS: a mutual interplay. *Redox Biol* 6:260–271
- de Loura SC, Silva Dde F, DeanaAM PRA, Souza AP, Gomes MT et al (2015) Tissue responses to postoperative laser therapy in diabetic rats submitted to excisional wounds. *PLoS One* 10:e0122042
- Loevschall H, Arenholt-Bindslev D (1994) Effect of low level diode laser irradiation of human oral mucosa fibroblasts in vitro. *Lasers Surg Med* 14(4):347–354
- Avci P, Gupta A, Sadasivam M, Vecchio D, Pam Z, Pam N, Hamblin MR (2013) Low-level laser (light) therapy (LLLT) in skin: stimulating, healing, restoring. *Semin Cutan Med Surg* 32:41–52
- Lapchak PA, De Taboada L (2010) Transcranial near infrared laser treatment (NILT) increases cortical adenosine-5'-triphosphate (ATP) content following embolic strokes in rabbits. *Brain Res* 1306:100–105
- Hopkins JT, McLoda TA, Seegmiller JG, David Baxter G (2004) Low-level laser therapy facilitates superficial wound healing in humans: a triple-blind, sham-controlled study. *J Athl Train* 39(3): 223–229
- Amaroli A, Agas D, Laus F, Cuteri V, Hanna R, Sabbieti MG, Benedicenti S (2018) The effects of photobiomodulation of 808 nm diode laser therapy at higher fluence on the in vitro osteogenic differentiation of bone marrow stromal cells. *Front Physiol* 9: 123. <https://doi.org/10.3389/fphys.2018.00123>
- Skopin MD, Molitor SC (2009) Effects of near-infrared laser exposure in a cellular model of wound healing. *Photodermatol Photoimmunol Photomed* 25(2):75–80

14. Szymanska J, Goralczyk K, Klawe JJ, Lukowicz M, Michalska M, Goralczyk B, Zalewski P et al (2013) Phototherapy with low-level laser influences the proliferation of endothelial cells and vascular endothelial growth factor and transforming growth factor-beta secretion. *J Physiol Pharmacol* 64(3):387–391
15. Peplow PV, Chung TY, Baxter DB (2010) Laser photobiomodulation of proliferation of cell in culture: a review of human and animal studies. *Photomed Laser Surg* 28(S1):S3–S40
16. Hawkins D, Abrahamse H (2007) Influence of broad-spectrum and infrared light in combination with laser irradiation on the proliferation of wounded skin fibroblasts. *Photomed Laser Surg* 25(3):159–169
17. Amaroli A, Ravera S, Parker S, Panfoli I, Benedicenti A, Benedicenti S (2016) 808-nm laser therapy with a flat-top handpiece photobiomodulates mitochondria activities of *Paramecium primaurelia* (protozoa). *Lasers Med Sci* 31(4):741–747
18. Amaroli A, Ravera S, Parker S, Panfoli I, Benedicenti A, Benedicenti S (2015) The protozoan *Paramecium primaurelia* as a non-sentient model to test laser light irradiation: the effects of an 808 nm infrared laser diode on cellular respiration. *Altern Lab Anim* 43(3):155–162
19. Amaroli A, Parker S, Dorigo G, Benedicenti A, Benedicenti S (2015) *Paramecium*: a promising non animal bioassay to study the effect of 808 nm infrared diode laser photobiomodulation. *Photomed Laser Surg* 33(1):35–40
20. Benvenuto F, Voci A, Carminati E, Gualandi F, Mancardi G, Uccelli A, Vergani L (2015) Human mesenchymal stem cells target adhesion molecules and receptors involved in T cell extravasation. *Stem Cell Res Ther* 6:245
21. Wang HZ, Chang CH, Lin CP, Tsai MC (1996) Using MTT viability assay to test the cytotoxicity of antibiotics and steroid to cultured porcine corneal endothelial cells. *J Ocul Pharmacol Ther* 12(1):35–43
22. Vergani L, Vecchione G, Baldini F, Grasselli E, Voci A, Portincasa P, Ferrari PF et al (2017) Polyphenolic extract attenuates fatty acid-induced steatosis and oxidative stress in hepatic and endothelial cells. *Eur J Nutr*. <https://doi.org/10.1007/s00394-017-1464-5>
23. Wiechelmann KJ, Braun RD, Fitzpatrick JD (1988) Investigation of the bicinchoninic acid protein assay: identification of the groups responsible for color formation. *Anal Biochem* 175(1):231–237
24. Vecchione G, Grasselli E, Voci A, Baldini F, Grattagliano I, Wang DQ, Portincasa P et al (2016) Silybin counteracts lipid excess and oxidative stress in cultured steatotic hepatic cells. *World J Gastroenterol* 22(26):6016–6026
25. Iguci H, Kojo S, Ikeda M (1993) Lipid peroxidation and disintegration of the cell membrane structure in cultures of rat lung fibroblasts treated with asbestos. *J Appl Toxicol* 13(4):269–275
26. Green LC, Wagner DA, Glogowski J, Skipper PL, Wishnok JS, Tannenbaum SR (1982) Analysis of nitrate, nitrite, and [15N] nitrate in biological fluids. *Anal Biochem* 126(1):131–138
27. Liang CC, Park AY, Guan JL (2007) In vitro scratch assay: a convenient and inexpensive method for analysis of cell migration in vitro. *Nat Protoc* 2(2):329–333
28. Laemmli UK (1970) Cleavage of structural proteins during the assembly of the head of bacteriophage T4. *Nature* 227(5259):680–685
29. Towbin H, Staehelin T, Gordon J (1979) Electrophoretic transfer of proteins from polyacrylamide gels to nitrocellulose sheets: procedure and some applications. *Proc Natl Acad Sci U S A* 76(9):4350–4354
30. Ravera S, Vaccaro D, Cuccarolo P, Columbaro M, Capanni C, Bartolucci M, Panfoli I et al (2013) Mitochondrial respiratory chain complex I defects in Fanconi anemia complementation group A. *Biochimie* 95(10):1828–1837
31. Hinkle PC (2005) P/O ratios of mitochondrial oxidative phosphorylation. *Biochim Biophys Acta* 1706(1–2):1–11
32. Lubart R, Eichler M, Lavi R, Friedman H, Shainberg A (2005) Low-energy laser irradiation promotes cellular redox activity. *Photomed Laser Surg* 23(1):3–9
33. Chen AC, Arany PR, Huang YY, Tomkinson EM, Sharma SK, Kharkwal GB, Saleem T et al (2011) Low-level laser therapy activates NF- $\kappa$ B via generation of reactive oxygen species in mouse embryonic fibroblasts. *PLoS One* 6(7):e22453
34. Di Meo S, Reed TT, Venditti P, Victor VM (2016) Harmful and beneficial role of ROS. *Oxidative Med Cell Longev* 2016:7909186
35. Eelen G, de Zeeuw P, Simons M, Carmeliet P (2015) Endothelial cell metabolism in normal and diseased vasculature. *Circ Res* 116(7):1231–1244
36. Gerasimovskaya EV, Woodward HN, Tucker DA, Stenmark KR (2008) Extracellular ATP is a pro-angiogenic factor for pulmonary artery vasa vasorum endothelial cells. *Angiogenesis* 11(2):169–182
37. Karu TI, Pyatibrat LV, Afanasyeva NI (2004) A novel mitochondrial signaling pathway activated by visible-to-near infrared radiation. *Photochem Photobiol* 80(2):366–372
38. Brookes PS, Yoon Y, Robotham JL, Anders MW, Sheu SS (2004) Calcium, ATP, and OS: a mitochondrial love-hate triangle. *Am J Phys Cell Phys* 287(4):C817–C833